Short Article

Structure

Crystal Structure of a Soluble Fragment of the Membrane Fusion Protein HlyD in a Type I Secretion System of Gram-Negative Bacteria

Graphical Abstract

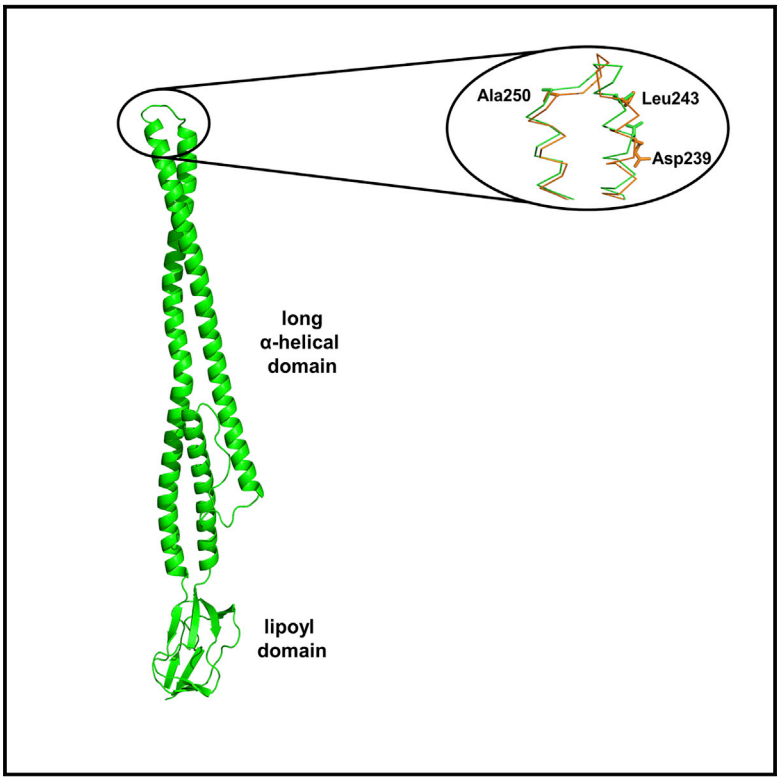

Authors

Jin-Sik Kim, Saemee Song, Minho Lee, Seunghwa Lee, Kangseok Lee, Nam-Chul Ha

Correspondence

hanc210@snu.ac.kr

In Brief

E. coli HlyD in T1SS has been solved, revealing a long α-helical domain with a structural flexibility. The structure also provides a structural blueprint for understanding T1SS in pathogenic Gram-negative bacteria.

Highlights

- Crystal structure of a soluble part of HlyD has been solved
- HlyD has a long α-helical domain consisting of three α helices
- α-Helical domain exhibits an α-helical tip region, which is functionally important
- Structural parallels in T1SS with tripartite multidrug efflux pump are suggested

Kim et al., 2016, Structure *24*, 477–485
March 1, 2016
http://dx.doi.org/10.1016/j.str.2015.12.012

Structure
Short Article

Crystal Structure of a Soluble Fragment of the Membrane Fusion Protein HlyD in a Type I Secretion System of Gram-Negative Bacteria

Jin-Sik Kim,[1,3] Saemee Song,[1,3] Minho Lee,[2] Seunghwa Lee,[2] Kangseok Lee,[2] and Nam-Chul Ha[1,*]
[1]Department of Agricultural Biotechnology, Center for Food Safety and Toxicology, Center for Food and Bioconvergence, Research Institute for Agricultural and Life Sciences, Seoul National University, Room #200-1041, 1 Gwanak-ro, Gwanak-gu, Seoul 151-921, Republic of Korea
[2]Department of Life Science, Chung-Ang University, Seoul, 156-756 Republic of Korea
[3]Co-first author
*Correspondence: hanc210@snu.ac.kr
http://dx.doi.org/10.1016/j.str.2015.12.012

SUMMARY

The protein toxin HlyA of *Escherichia coli* is exported without a periplasmic intermediate by the type I secretion system (T1SS). The T1SS is composed of an inner membrane ABC transporter HlyB, an outer-membrane channel protein TolC, and a membrane fusion protein HlyD. However, the assembly of the T1SS remains to be elucidated. In this study, we determine the crystal structure of a part of the C-terminal periplasmic domain of HlyD. The long α-helical domain consisting of three α helices and a lipoyl domain was identified in the crystal structure. Based on the HlyD structure, we modeled the hexameric assembly of HlyD with a long α-helical barrel, which formed a complex with TolC in an intermeshing cogwheel-to-cogwheel manner, as observed in tripartite RND-type drug efflux pumps. These observations provide a structural blueprint for understanding the type I secretion system in pathogenic Gram-negative bacteria.

INTRODUCTION

Gram-negative bacteria have developed sophisticated secretion systems due to their characteristic double-layer membranes. Secretion of cytotoxin α-hemolysin (HlyA) in many uropathogenic strains of *Escherichia coli* is mediated by the protein complex Hly translocator, belonging to the type I secretion system (T1SS) (Lewis, 2000; Noegel et al., 1979). The 108-kDa HlyA acts on host cell membrane including pore formation on the cell membranes and association with outer-membrane vesicles, which is an essential step for the bacteria in initiating the infectious process (Welch et al., 1981). The T1SS is widely spread in pathogenic Gram-negative bacteria. Specifically, the food-borne bacteria *Vibrio vulnificus* secretes protein toxins through this system, which is crucial for the pathogenesis of the bacteria (Choi et al., 2002).

The Hly translocator comprises HlyB, HlyD, and TolC (Schulein et al., 1994). The inner membrane protein HlyB is a member of the ATP-binding cassette (ABC) transporter family, and transports HlyA from the cytosol utilizing ATP hydrolysis (Schmitt et al., 2003; Wang et al., 1991). TolC is the outer-membrane channel protein and is often the final portal in the pathways of protein toxin transport or export of unwanted molecules (Koronakis et al., 2000). HlyD belongs to membrane fusion protein (MFP) family, and is also called a periplasmic adaptor protein (Lee et al., 2012). HlyD forms a continuous channel by docking to the outer-membrane protein, TolC. This ternary complex spans the entire cell envelope including two membranes and the periplasm (Thanabalu et al., 1998).

HlyD is predicted to have a small N-terminal cytoplasmic tail, a transmembrane region, and a C-terminal large periplasmic domain, whose three-dimensional structure remains mostly unknown (Balakrishnan et al., 2001). However, it has been structurally characterized based on its functional homologs, AcrA, MacA, and CusB (Mikolosko et al., 2006; Su et al., 2009, 2011; Yum et al., 2009), which are the MFPs in the multidrug efflux pump AcrA-AcrB-TolC, the macrolide-specific pump MacA-MacB-TolC, and the heavy metal efflux pump CusB-CusA-CusC. The periplasmic domains of AcrA, MacA, and CusB commonly comprise a membrane proximal (MP) domain, a β-barrel domain, a lipoyl domain, and an α-helical domain, which are linearly arranged (Akama et al., 2004; Higgins et al., 2004; Mikolosko et al., 2006; Su et al., 2009; Symmons et al., 2009; Yum et al., 2009). All of the α-helical domains are responsible for binding to their cognate outer-membrane channel protein (Bavro et al., 2008; Gerken and Misra, 2004; Kim et al., 2010; Lobedanz et al., 2007; Xu et al., 2010, 2011a, 2011b). The α-helical domains of AcrA and MacA consist of coiled-coil α hairpins with different lengths (Mikolosko et al., 2006; Yum et al., 2009), except the CusB α-helical domain that is folded into a three-helix bundle structure (Su et al., 2009, 2011). Crystal structures, combined with genetic studies, have established that MacA and CusB exhibit a funnel-like hexameric assembly in the functional state (Xu et al., 2010, 2011b; Yum et al., 2009; Zgurskaya et al., 2011).

Recently, the electron microscopy structures of the AcrAB-TolC complex have been determined by two independent research groups, revealing that AcrA creates a funnel-like hexamer on AcrB and forms an α barrel consisting of six α hairpins with the α-helical domain (Du et al., 2014; Kim et al., 2015). The AcrA α barrel performs direct interactions

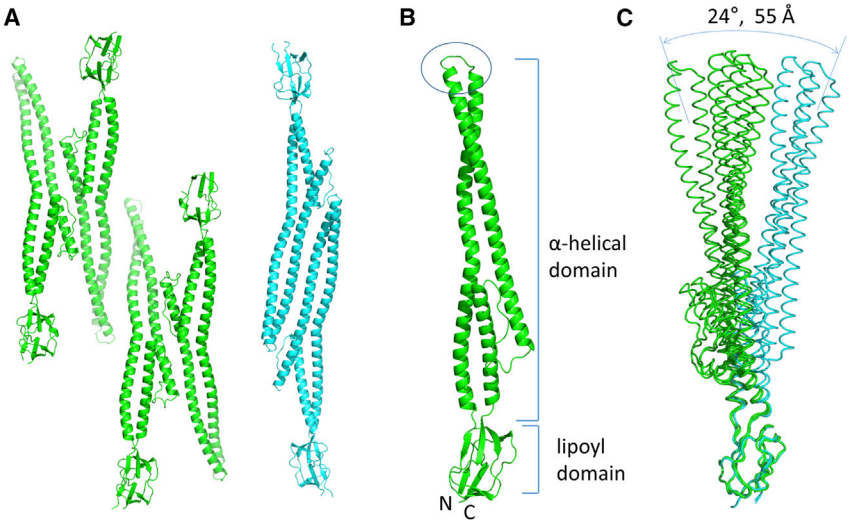

Figure 1. Overall Structure of HlyD

(A) The asymmetric units of HlyD. The asymmetric unit of the crystals grown at pH 6.5 is shown on the left (green; four protomers), while that of the crystals grown at pH 7.8 is noted on the right (cyan; two protomers).

(B) The overall structure of the HlyD protomer consisting of an α-helical domain and lipoyl domain. The α-helical tip region is indicated by a circle.

(C) The six protomers in the asymmetric units of two crystal forms were superposed on the lipoyl domain as a reference. The greatest difference is 24° wide and 55 Å distant. The color scheme is identical to that used in (A).

with the TolC trimer using both tip regions from the α barrels of the two cylindrical proteins (Song et al., 2015). HlyD has low sequence similarity with AcrA, MacA, and CusB, and no HlyD crystal structure is available, which hampers T1SS studies. In this study, we present the crystal structure of a soluble fragment of HlyD, providing insight into the assembly of the T1SS.

RESULTS

Crystallization and Structural Determination of *E. coli* HlyD

Sequence analysis of *E. coli* HlyD suggested a transmembrane helix (residues 60–80) and a C-terminal AcrA homologous region (residues 81–478) (Balakrishnan et al., 2001). To facilitate the structural determination, we expressed several fragments of HlyD and found a fragment (residues 81–383) that exhibited an acceptable expression level for further analyses. The protein was trimmed by limited proteolysis using trypsin, and subsequent N-terminal sequencing led to the determination of a proteolysis-resistant fragment of HlyD. The HlyD fragment covers residues 96–372, corresponding to the central part of the C-terminal AcrA homologous region. We obtained two crystal forms at different pH using this fragment. The crystal structure of the crystals grown at pH 6.5 was determined by averaging Zn-anomalous signals from five individual Zn-soaked crystals at 2.3 Å resolution (Cha et al., 2012; Liu et al., 2013) (Figure 1A, left). The crystal belongs to the space group $P2_12_12_1$ and contained four protomers in the asymmetric unit, with 56.8% of the solvent contents. The final refined models contained residues 96–361 of the protein, with R_{work} and R_{free} values of 22.7 and 26.4, respectively (Table 1). The other crystal structures grown at pH 7.8 with a different unit cell dimensions were solved at a 2.5 Å resolution (75% of the solvent contents) using the molecular replacement method with the structure solved initially as a search model (Figure 1A, right). The asymmetric unit of the crystal contained two protomers. The final refined models contained residues 94–363 of the protein, with R_{work} and R_{free} values of 23.5 and 27.4, respectively (Table 1).

Overall Structure of HlyD

The overall structures of the protomers in both crystals are similar. The fragment is largely divided into two parts: α-helical and lipoyl domains (Figure 1B). Regions close to both ends of the HlyD fragment form the lipoyl domain and the remaining middle region forms the α-helical domain. Through structural superposition of the six protomers observed in two crystal forms using the lipoyl domains as a reference, significant conformational flexibility between the two domains was found (Figure 1C). The maximum difference was ~24° overall and ~55 Å at the α-helical tip regions. The extent of the conformational flexibility of the α-helical domain in HlyD was far greater than that of the AcrA structure (~15° and 21 Å, respectively) (Mikolosko et al., 2006). The motion of the α-helical domain with respect to the other domains seems to be necessary in oligomerization (or hexamerization) of AcrA (Xu et al., 2011a). Thus, the structural flexibility of HlyD suggests that the interdomain motion occurs during oligomerization in the functional assembly.

α-Helical Domain

The remarkable feature of HlyD is the highly elongated α-helical domain, which is 115 Å long (Figure 2A). Compared with the corresponding α-helical domains of EmrA, MacA, AcrA, and CusB, HlyD showed a length similar to that of the longest EmrA (127 Å) (Figure 2A) (Hinchliffe et al., 2014). EmrA is the MFP in the EmrAB-TolC efflux pump (Hinchliffe et al., 2014). The α-helical domain of HlyD consists of three α helices (α1, α2, α3) and two connecting loops (L1 and L2), which is unique because most α-helical domains of most MFPs consist of two α helices. α Helices α1 (residues 132–162) and α2 (residues 181–244) are connected by a loop (L1; 163–180) in a zigzag manner (Figure 2A). This zigzag region might be associated with the structural flexibility of the long α-helical domain.

The third helix, α3 (residues 251–325), is longer than α1 and α2, which allows anti-parallel coiled-coil interactions with both α1 and α2 (Figure 2A). The α3 helix has a slight bend in the middle of the long α helix. The upper-half region (residues 251–294) of α3 forms a coiled-coil α-helical hairpin with α2, where loop L2 connects α2 and α3 at the tip region of the α-helical domain. This α-helical hairpin structure of HlyD is reminiscent of the α hairpins of other MFPs (Figure 2A). The lower-half region (residues 252–325) of α3 and α1 formed coiled-coil α helices (Figure 2A).

Table 1. X-Ray Data Collection and Refinement Statistics

Dataset	pH 7.8 Crystal Form	pH 6.5 Crystal Form (Zn-Soaked, Averaged)
Data Collection		
Wavelength (Å)	0.99998	–
Resolution limit (Å)	20.0–2.2 (2.24–2.2)	37.2–2.3 (2.39−2.3)
Space group	$P2_12_12_1$	$P2_12_12_1$
Unit cell (Å)	a = 77.6, b = 93.2, c = 163.4	a = 80.9, b = 94.5, c = 181.4
Reflections[a]	352,687	1,852,494
Unique	58,658	59,484
Redundancy	6.0 (2.4)	65.8 (63.2)
R_{sym} (%)[a]	8.2 (36.7)	28.9 (62.7)
Completeness (%)[a]	95.3 (87.0)	100 (100)
Average I/σ[a]	21.1 (2.2)	21.6 (9.7)
Refinement		
Resolution range (Å)	20–2.5	37.2–2.3
R factor (%)	23.54	22.67
R_{free} (%)[b]	27.44	26.36
Average B value (Å^2)	65.8	44.2
Wilson B value (Å^2)	46.11	27.38
Rmsd for bonds (Å)	0.004	0.004
Rmsd for angles (°)	0.831	0.758
Ramachandran plot		
Most favored	98.85	99.23
Additionally favored	1.15	0.67
Coordinate error (Å)	0.39	0.35
PDB ID	5C21	5C22

[a]The numbers in parentheses are statistics for the highest-resolution shell.
[b]R_{free} was calculated with 5% of the dataset.

Sequence alignment of the HlyD homolog proteins from diverse bacteria revealed that the α-helical domains consist of 193 or 194 amino acids with a high sequence homology. Only one gap was located within the loop L1 region, which seems not to result in significant variation in the overall structure of this domain. Thus, HlyD commonly has this α-helical domain consisting of the three α helices, indicating that the unique arrangement in this domain serves a functional role in the T1SS (Figure 2B).

We next noted the loop L2 in the α-helical tip region of HlyD, since the α-helical tip region of AcrA is responsible for binding to TolC (Kim et al., 2010; Song et al., 2015). In particular, the RLS motif at this region of AcrA was crucial for binding to TolC and function. We superposed the α-helical tip structures of HlyD and AcrA and identified the parallel motif in HlyD (Figures 3A and 2B). The leucine residue in the RLS motif is the most conserved among all MFP sequences. Consistently, the leucine residue in the motif is conserved in HlyD, while the arginine and serine residues are replaced in a homologous manner. We tested the functionality of these residues, especially the first Asp239 and Leu243 residues of HlyD. Upon mutation (D239A or L243A) at these residues, both secretion of HlyA by the bacteria to the medium and the hemolytic ability (Figures 3B [top] and 3C) were abolished even though the cellular expression levels of HlyA and HlyD were not changed (Figure 3B, bottom).

We subsequently carried out an in vivo crosslinking experiment to examine whether the absence of the secretion of HlyA results from the reduced affinity of HlyD to TolC. To detect the interaction between TolC and HlyD proteins, we compared the pull-down efficiency of TolC and HlyD or its mutants (HlyD-D239A and HlyD-L243A) after treatment of the agent dithiobis(succinimidyl propionate) (DSP) to the live cells. DSP is a common chemical crosslinking agent with a fixed 12-Å spacer arm to stabilize the transient protein complexes. As shown in Figure 3D, the crosslinking efficiency of HlyD-D239A and HlyD-L243A to TolC were 66% and 42% of that of wild-type HlyD to TolC, respectively. These results show that the tip region of HlyD affects the binding of HlyD to TolC. Combined with the location of the tip region in the crystal structure, our findings suggest that the α-helical tip region of HlyD plays a crucial role in the secretion of HlyA through the binding to TolC, sharing the mode of binding to OMP (or TolC) with AcrA (Song et al., 2015).

Lipoyl Domain

A simple sequence alignment failed to predict the presence of a lipoyl domain in HlyD. However, the crystal structure of HlyD displayed a lipoyl domain connected to the α-helical domain, as observed in all MFPs. The HlyD lipoyl domain consists of residues 96–131 and 326–361, and the structure of the domain is located in the same fold as those from the other MFPs (Figure 4A). The structural superposition with the AcrA lipoyl domain showed a slight variation (Figure 4B; root-mean-square deviation [rmsd] 2.15 Å between 48 Cα atoms).

In the hexameric funnel-like models of AcrA and MacA, the lipoyl domains form a doughnut-like arrangement that has a hole in the center. The hole is the narrowest region of the central channel in the pump complex (Kim et al., 2015; Xu et al., 2011b). When the HlyD lipoyl domain was superposed on the AcrA lipoyl domains in the hexameric model, a similar channel was observed in the center of the doughnut-like structure consisting of the HlyD lipoyl domains.

Modeling the HlyD Hexamer

Given the common structural motif in the α-helical tip region of HlyD with MFPs in the RND-type efflux pumps, a hexameric assembly and intermeshing cogwheel-like interaction with TolC was proposed (Lee et al., 2012). To test whether the HlyD hexamer can be formed, we constructed a forced oligomer (or hexamer) of the HlyD fragment by making a fusion protein with Hfq from *E. coli* that forms a stable hexamer in a ring arrangement (Sauter et al., 2003) (Figure 5A). Experiments using a size-exclusion chromatographic column showed that the Hfq-fused HlyD protein makes a complex with a chimera protein, called MacA-TolCα hybrid, which contains the TolC α-helical tip region and a hexameric protein, MacA (Xu et al., 2011b) (Figure 5B). However, the HlyD fragment did not make a complex with the MacA-TolCα hybrid without fusion with Hfq (data not shown). Since MacA-TolCα hybrid was tightly bound to MacA and AcrA hexamer in vitro (Xu et al., 2011a, 2011b), the chimera protein was able to mimic the TolC protein in the open state. Our findings indicate the importance of the oligomerization of HlyD for binding

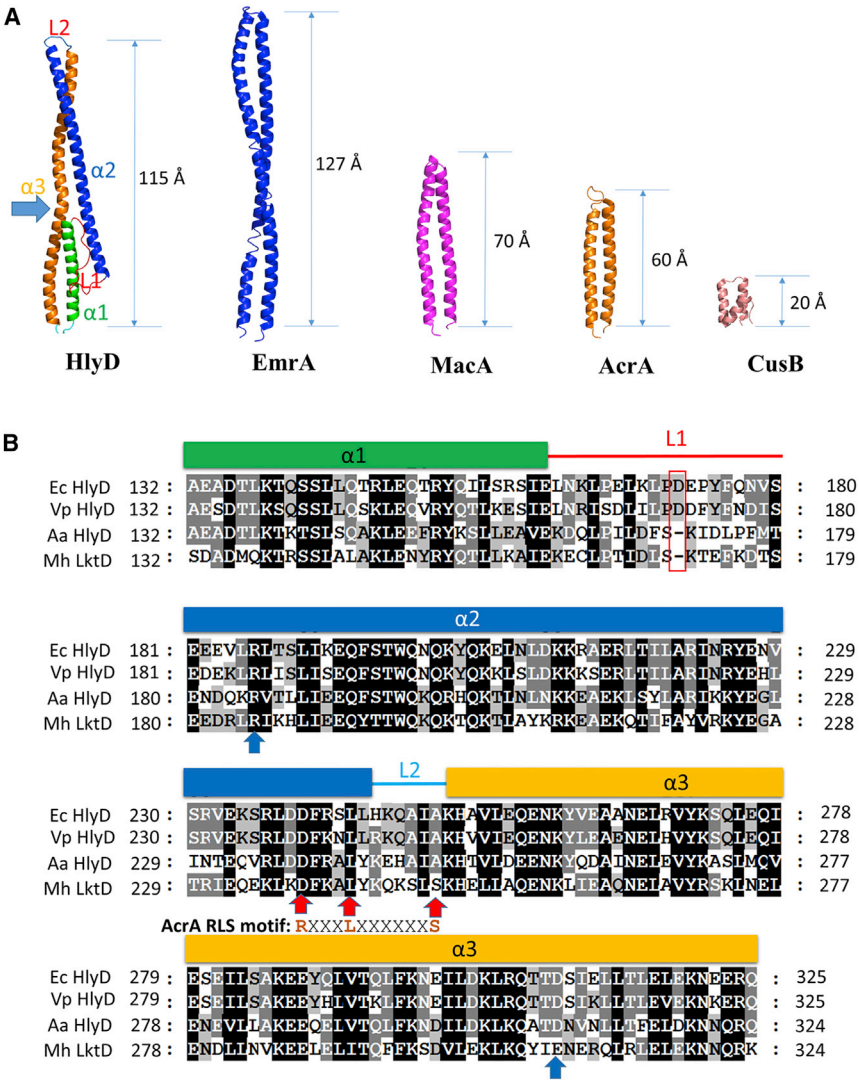

Figure 2. Structure of the α-Helical Domain

(A) Comparison of α-helical domains from HlyD, EmrA, MacA, AcrA, and CusB. The heights of the domains are indicated. In the HlyD structure, α1, L1, α2, L2, and α3 are labeled with different colors (green, red, blue, cyan, and orange, respectively). The slight bend observed in α3 is indicated by an arrow.

(B) Sequence alignment of the α-helical domains of the HlyD homologs. The secondary structural elements are shown above the sequence in the same color scheme as in (A). The gap in L1 is shown in a red box. The blue arrows indicate the Arg186 and Asp309 residues. The AcrA RLS motif is displayed under the corresponding sequence, with the red arrows indicating the conserved amino acids. Ec, *Escherichia coli*; Vp, *Vibrio parahaemolyticus*; Aa, *Actinobacillus actinomycetemcomitans*; Mh, *Mannheimia haemolytica*.

to TolC, and further suggest that the rest region of the HlyD fragment may help oligomerization of the protein in cells.

Based on the hexameric nature of HlyD, we constructed a hexameric model of HlyD as a candidate assembly, based on the crystal structure of *E. coli* MacA (Yum et al., 2009). As substantial flexibility between the domains was observed in the crystal structure, the α-helical domain and lipoyl domains were separately superposed on the corresponding domains of MacA (Figure 3). The α-helical domain of HlyD exhibited a long cylinder-like structure with a belt around the middle of the barrel (~140 Å tall). The six-bladed cogwheel-like structure was observed in the tip region of the α barrel. The internal diameter was ~40 Å, which was sufficiently large to allow passage of the polypeptide chain. The main force for the hexamerization of HlyD appears to be the coiled-coil α-helical interaction between α2 and the α3 of the neighboring molecules, according to the model (Figure 6A). We found a conserved Arg186 residue in α2 at this binding interface (Figures 2B and 6B). According to a previous study, the mutation of Arg186 to Ala abolished the function of HlyD in vivo (Lee et al., 2012). Interestingly, the conserved Asp309 residue in α3 is located near Arg186, producing electrostatic interaction in the hexameric model, which increases the plausibility of this model (Figures 2B and 6B). The lipoyl domains of HlyD, superposed on the AcrA hexamer, displayed a doughnut-like shape with an internal pore size of ~20 Å, through which an unfolded polypeptide chain could pass. However, more evidence is needed to prove the hexameric model of HlyD.

DISCUSSION

Many proteins in Gram-negative bacteria are secreted via the T1SS. In particular, the T1SS of uropathogenic *E. coli* and *V. vulnificus* plays a critical role in their pathogenicity. In this study, we provided the first structural feature of the MFP in the T1SS with a soluble fragment of HlyD. We observed a significant structural flexibility of the α-helical domain with respect to the lipoyl domain. We also found that the HlyD fragment in a forced hexameric form can interact with the TolC α-helical tip region. A model of the HlyD hexamer was built based on the arrangement of the hexameric MFP in the complex. The modeled HlyD hexamer shared the six-bladed cogwheel structure with other MFPs in RND-type drug efflux pumps. We provided evidence supporting that the residues in the cogwheel were important for the function of HlyD, like MFPs in RND-type drug efflux pumps (Song et al., 2015). These findings suggest that the oligomerization of HlyD and the α-helical tip region of the α-helical domain plays an important role in TolC binding. However, a binary or ternary complex structure containing the full-length HlyD protein may be required to elucidate the assembly of HlyD in the functional state.

The HlyD structure presented in this study does not cover the full-length protein. Thus, the structure of the N-terminal 95 residues (residues 1–95) and C-terminal ~100 residues (residues 372–478) is still unknown. Since these missing parts of HlyD do

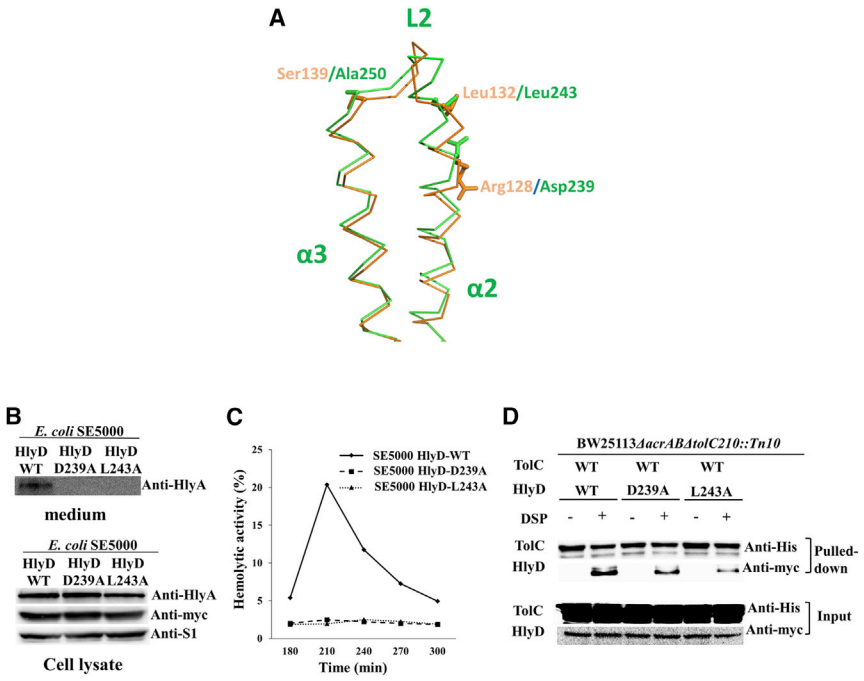

Figure 3. The α-Helical Tip Region

(A) Structural superposition of the α-helical tip regions of HlyD (green) and AcrA (orange), displayed as Cα traces. The residues in the RLS motifs are shown in the stick representations.

(B) *E. coli* SE5000 expressing wild-type (WT) or mutant HlyD. The HlyA protein in the medium (top) was visualized by immunoblot using anti-HlyA antibody. The cellular expression level of the myc-tagged HlyA is shown relative to that of control protein S1 (bottom).

(C) Hemolytic activity of *E. coli* SE5000 expressing WT or mutant HlyD. The absorbance values at 450 and 543 nm were detected using a UV-visible spectrophotometer, and hemolytic activities were calculated according to the formula reported previously (Lee et al., 2012).

(D) Interaction between TolC and HlyD in vivo, detected by using a chemical crosslinking agent DSP on an *E. coli* strain (BW25113*ΔacrAB ΔtolC210::Tn10*) coexpressing HlyB, C-terminal hexahistidine-tagged TolC and c-Myc-tagged HlyD, or one of the HlyD mutants (D239A and L243A). All cultures were treated with (+) or without (–) DSP, and affinity-purified TolC and crosslinked HlyD proteins were analyzed by SDS-PAGE and immunoblotted using a monoclonal antibody for detection of TolC or HlyD proteins.

not have significant homology to other MFPs, simple sequence alignment cannot provide significant insight regarding the structures of these domains. However, the structural information of these sequences could be obtained from EmrA, which is a functional homolog of the EmrAB-TolC pump. EmrA has a long α-helical hairpin, lipoyl domain, and β-barrel domain (Hinchliffe et al., 2014). However, unlike other MFPs, EmrA lacks an MP domain. The major facilitator superfamily member EmrB has a very small periplasmic domain, like typical ABC-type transporters such as HlyB. Given the structural similarity to EmrA, it is very likely that HlyD has a β-barrel domain but not an MP domain. Since HlyD has a predicted transmembrane helix (Balakrishnan et al., 2001), HlyD is directly attached to the inner membrane through this helix without the MP domain.

In a previous chimeric study of HlyD, a motif containing Arg186, Leu190, and Thr197 was suggested as a TolC binding site since a single mutation at these residues totally abolished the binding of HlyD to TolC (Lee et al., 2012). However, this study revealed that all the residues are located in the side of α-helical domain, but not in the α-helical tip region that is presumably important in binding to TolC. Since the side region of the α-helical domain is located at the putative oligomerization interface, the residues appear to be important in the oligomerization of HlyD that is a prerequisite for recruitment to TolC (Letoffe et al., 1996).

Due to the extensive structural studies on tripartite drug efflux pumps, the complex structure in the functional state and its working mechanism are now being elucidated. Compared with these efflux pumps, the T1SS still has many uncertainties. The oligomerization numbers of HlyD and the supramolecular assembly of the components are still unclear. Here, we presented the HlyD structure and a model of the HlyD hexamer as a candidate oligomeric assembly, and found structural parallels with the multidrug efflux pumps. Our findings are the first step toward elucidating the assembly of T1SS at the molecular level, which is required to design drugs counteracting the toxin secretion of pathogenic bacteria.

EXPERIMENTAL PROCEDURES

Plasmid Construction

DNA fragments encoding HlyD of *E. coli* (residues 81–478, 81–383, 81–301, and 96–372) were amplified using PCR. The DNA fragment was inserted into the NcoI and XhoI sites of a pPROEX-HTA vector (Invitrogen). To construct the Hfq-fused HlyD fragment (81–383) we amplified the *hfq* gene of *E. coli*, after which the DNA fragment was digested with NcoI and EcoRI and inserted at the same site of a pPET28a vector. The Hfq-cloned pET28a plasmid was digested with EcoRI and XhoI for ligation of the DNA encoding HlyD (residues 81–383) that was amplified by PCR. The final plasmid, pET28a-Hfq-HlyD, carries Hfq-fused and C-terminal hexahistidine-tagged HlyD (residues 81–383).

Expression and Purification

HlyD fragments (residues 1–472, 81–479, 81–383, 81–301, and 96–372) with N-terminal His-tag were expressed in *E. coli* strain BL21 (DE3) in Luria-Bertani (LB) medium at 37°C until the OD_{600} reached 0.5. Cultures were induced by adding 0.5 mM isopropyl-D-1-thiogalactopyranoside (IPTG) and cultured at 30°C for 6 hr. The cells were harvested by centrifugation after induction and stored at −80°C until use. To purify the protein, we resuspended the cells in lysis buffer consisting of 20 mM Tris (pH 8.0), 150 mM NaCl, and 2 mM 2-mercaptoethanol, and disrupted them by sonication. After removing the cell debris by centrifugation at 19,000 × *g* for 30 min, the soluble lysate was subjected to immobilized metal-ion affinity chromatography using Ni-nitrilotriacetic acid (NTA) resin (Qiagen). The resin was washed with the lysis buffer supplemented with 20 mM imidazole, and the hexahistidine-tagged HlyD protein was eluted with lysis buffer supplemented with 250 mM imidazole. At this stage, only two HlyD fragments (residues 81–383 and 96–372) were produced in sufficient amounts for the following purification and analysis steps. Fractions containing the HlyD protein were pooled, and the hexahistidine tag was then cleaved by treatment with recombinant tobacco

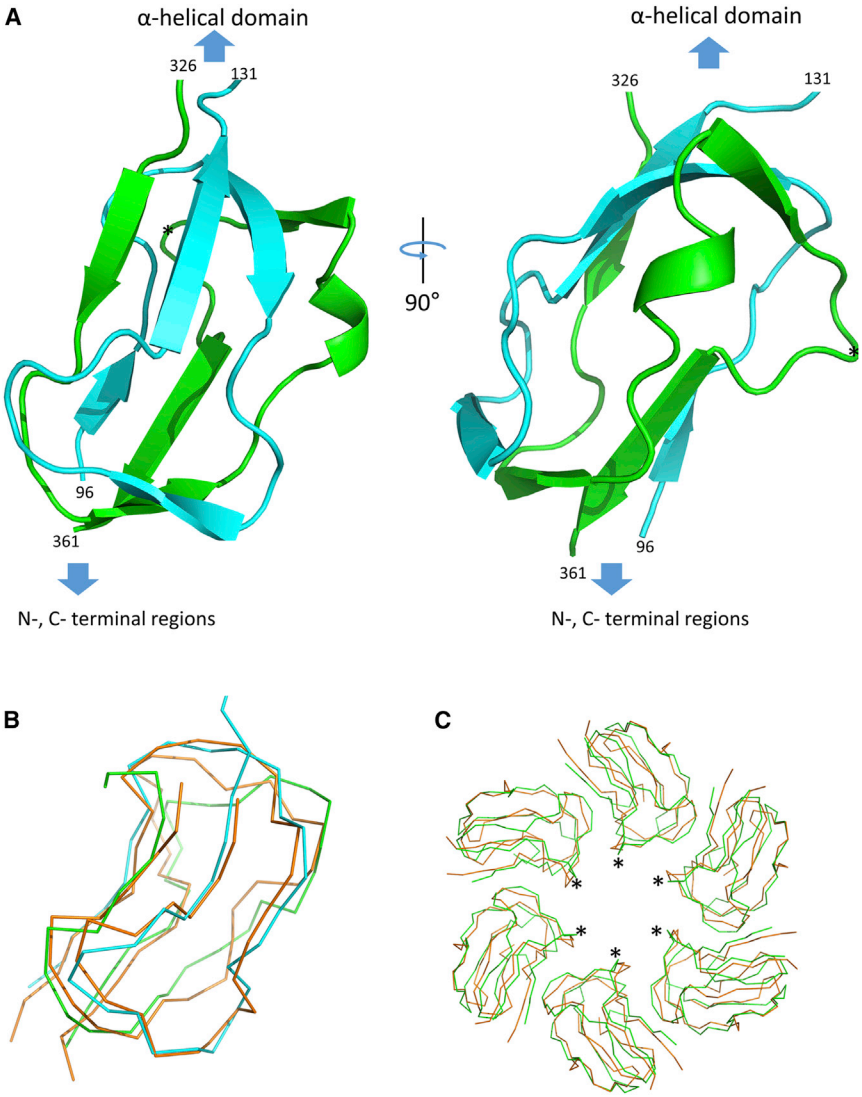

Figure 4. The Lipoyl Domain Structure

(A) Two orthogonal views of the lipoyl domain, displayed in ribbon representation. The first part (residues 96–131) is shown in cyan and the second part (residues 326–361) in green.

(B) Structural superposition of the HlyD lipoyl domain (cyan and green) onto one copy of the AcrA lipoyl domain (orange).

(C) The structural superposition of HlyD lipoyl domains (green) on the six copies of the AcrA lipoyl domains in the hexameric arrangement. The residues in the narrowest region are indicated by asterisks.

etch virus protease. The HlyD protein was then further purified using HiLoad Superdex 200 (GE Healthcare), pre-equilibrated with lysis buffer. The purified protein was concentrated and stored at −80°C until use. For production of the Hfq-fused HlyD fragment (81–383), Hfq-fused HlyD was expressed in *E. coli* C43(DE3) in LB medium including 50 μg/ml kanamycin at 37°C until the OD_{600} reached 0.6. Cultures were induced by adding 0.5 mM IPTG and cultured at 16°C for 12 hr. After being harvested, the cells were resuspended in lysis buffer consisting of 20 mM Tris (pH 8.0), 300 mM NaCl, and 2 mM 2-mercaptoethanol, and disrupted by sonication. After centrifugation, the lysate was applied to Ni-NTA resin as described above. The eluted protein from Ni-NTA resin was further purified using HiLoad Superdex 200 16/600, equilibrated with 20 mM Tris-HCl (pH 8.0) buffer including 150 mM NaCl and 2 mM 2-mercaptoethanol. The purified protein was concentrated and prepared fresh for the experiment. The MacA-TolCα hybrid protein was produced as previously described (Xu et al., 2011b).

Limited Proteolysis

The HlyD fragment (residues 81–383) was subjected to limited proteolysis to produce a more stable fragment. The purified HlyD fragment (1 mg) was treated with trypsin (0.1, 0.5, and 1 mg/ml) for 30 min at 37°C. A stable fragment with a ~10-kDa lower band on an SDS-polyacrylamide gel than the untreated protein band and the N-terminal residues were identified through Edman degradation. The C-terminal residues of the fragment were suggested by the apparent molecular weight of the gel fragment. The resulting fragment covered residues 96–372.

Crystallization

The HlyD fragment (residues 96–372) was concentrated to 15 mg/ml using a centrifugal filter concentration device (Millipore; 10 kDa cutoff). To obtain the pH 6.5 crystal form, we applied the vapor-diffusion hanging-drop method in a mother liquid containing 0.1 M sodium cacodylate (pH 6.5), 0.2 M calcium acetate, and 14% polyethylene glycol (PEG) 8000 at 14°C. To obtain the pH 7.8 crystal form, we applied the vapor-diffusion hanging-drop method in a mother liquid consisting of 0.1 M Tris (pH 7.8), 3% poly-γ-glutamic acid polymer (PGA-LM; ~400 kDa), and 14% PEG 400 at 14°C.

Data Collection and Structural Determination

To derivatize the crystal with Zn, we soaked the crystals (pH 6.5 form) in 10 mM $ZnCl_2$ for 6 hr. Phases were determined using the anomalous signals from the bound Zn ions in five Zn-soaked crystals (Cha et al., 2012). X-Ray diffraction data from the crystals were collected on an ADSC Q-270 CCD detector installed in beamline 7A of Pohang Accelerator Laboratory (Republic of Korea). The five datasets were scaled together using the program SCALA to amplify the anomalous signals by increasing the redundancy (Liu et al., 2013; Winn et al., 2011). The five Zn sites were identified using the program PHENIX (Echols et al., 2012), and produced a high-quality electron density map. Four molecules were found in the asymmetric unit, which corresponded to a solvent content of 56.8%. The model was constructed with the program Coot (Emsley et al., 2010). The R_{work} and R_{free} values of the final model at 2.3 Å resolution were 22.7 and 26.4, respectively. X-Ray diffraction data of the crystals grown at pH 7.8 were collected on an ADSC Q-315 CCD detector installed in beamline 5C of Pohang Accelerator Laboratory. The diffraction dataset was processed and scaled using the HKL-2000 package (Otwinosky and Minor, 1997). This HlyD structure was determined using the molecular replacement package MOLREP (Vagin and Teplyakov, 2010) with the Zn-bound structure (pH 6.5 crystal form) as a starting model. Model construction was performed with Coot (Emsley et al., 2010), and model refinement was conducted using the program PHENIX (Echols et al., 2012). Data collection and refinement statistics are summarized in Table S1.

Bacterial Strain and Construction for Detection of HlyA

The non-pathogenic *E. coli* strain SE5000 (*rpsL ara139*Δ*[lacIPOZYA]U169 recA57 thi*) was used for the in vivo study. Cells were grown at 37°C in LB medium including 10 mM $CaCl_2$ for the hemolytic assay. Plasmid pLG815 carried the *hlyBD* gene cloned from the wild-type pathogenic strain

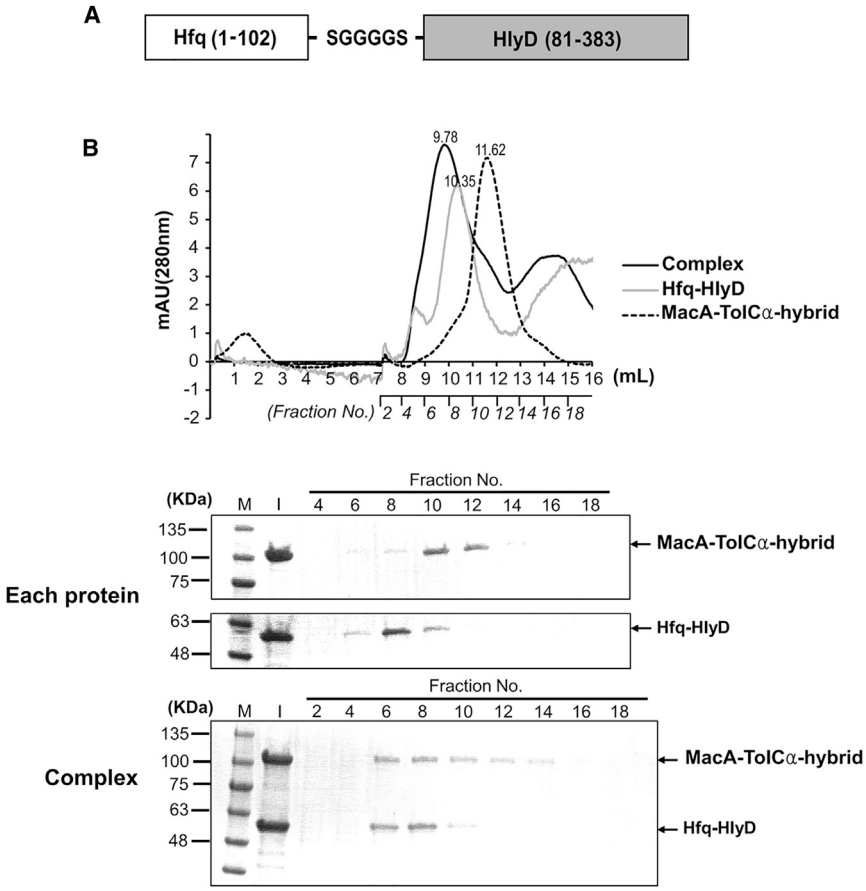

Figure 5. A Forced Hexamer of HlyD Binds to the TolC α-Helical Barrel Tip Region

(A) A bar diagram for the construction of Hfq-HlyD fusion protein. *E. coli* Hfq was fused to the HlyD fragment via a short linker consisting of serine and glycine residues as indicated.

(B) Elution profiles on a size-exclusion gel-filtration chromatographic column (Superdex 200 10/300) of Hfq-HlyD, MacA-TolCα hybrid, and their complex (top). Each fraction was further analyzed by SDS-PAGE (bottom). The elution volumes (9.78, 10.35, and 11.62 ml) are indicated above the peaks that correspond to 900, 690, and 380 kDa molecular size, respectively.

LE2001 (Mackman and Holland, 1984). Plasmid pLG813 was a pACYC derivative encoding the *hlyCA* genes (Kenny et al., 1992). Plasmid pLG815 HlyD C-*myc* encodes the C-terminal region of HlyD with a C-*myc* tag (Lee et al., 2012). pLG815 HlyD-D239A C-*myc* and HlyD-L243A C-*myc* were constructed using the overlap extension PCR method. The resulting PCR product was digested with AccI and XbaI and then ligated into the AccI and XbaI sites in HlyD C-*myc* to produce the plasmids described above. Primers used for plasmid generation are listed in Table S2.

Detection of HlyA

HlyA was detected from the medium and cell lysate, as described previously (Lee et al., 2012).

Measurement of Hemolytic Activity

The procedure for measuring the hemolytic activity of *E. coli* has been previously described (Bhakdi et al., 1984).

Crosslinking Experiment

The whole procedure for in vivo DSP-mediated crosslinking has been previously described (Thanabalu et al., 1998). *E. coli* BW25113*ΔacrABΔtolC210::Tn10* cells harboring pBluscriptII-HlyBD-myc or its derivatives (HlyD-D239A-myc and HlyD-L243-myc) and pTolC1 were grown in LB medium including appropriate antibiotics to OD_{600} = 0.7 and used for crosslinking experiments (Lee et al., 2012). Anti-His and anti-Myc monoclonal antibodies were used to detect TolC with C-terminal hexahistidine and HlyD with C-terminal c-Myc tags, respectively.

Size-Exclusion Chromatography

Size-exclusion chromatography for Hfq-HlyD fusion protein, AaMacA-TolCα hybrid protein, and their complex was performed at a flow rate of 0.5 ml/min on a Superdex S-200 HR 10/300 (GE Healthcare) pre-equilibrated with 20 mM Tris-HCl (pH 8.0), 150 mM NaCl, and 2 mM 2-mercaptoethanol. For

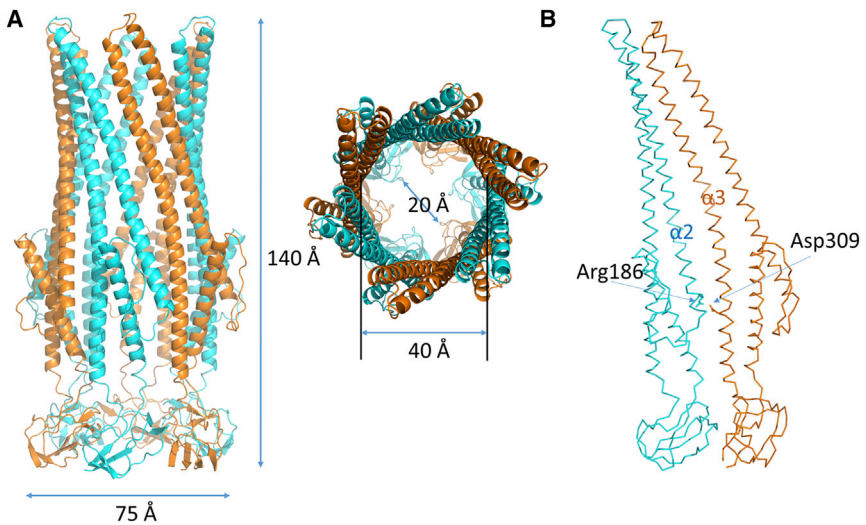

Figure 6. The Hexameric Model of HlyD

(A) Six HlyD protomers (cyan and orange) are assembled in side-by-side arrangement, which is observed in the funnel-like hexamers of MacA or AcrA. Each domain was independently superposed on the MacA or AcrA hexamer to construct the model. The overall dimension of the complex is indicated.

(B) The modeled interaction between two adjacent protomers. The intermolecular coiled-coil interaction between α2 and α3 is observed. The electrostatic interaction between Arg186 and Asp309 is observed in the model.

sufficient binding between Hfq-HlyD and AaMacA-TolC α-hybrid protein, 0.7 mg/ml AaMacA-TolC α hybrid protein was pre-incubated with the same concentration of Hfq-HlyD fusion protein for 4 hr at 4°C before injection onto the column. Six proteins (thyroglobulin, 669 kDa; ferritin, 440 kDa; aldolase, 158 kDa; conalbumin, 75 kDa; carbonic anhydrase, 29 kDa; RNase A, 13.7 kDa, aprotinin; 6.5 kDa) were used for molecular mass standards, and void volumes were measured with Blue Dextran (GE Healthcare). The peak elution volumes were used for the calculation of the standard curve equation Log MW = $-0.2041x + 4.9517$ (R^2 value for the curve fit = 0.9826). The eluted fractions from the column were characterized by SDS-PAGE and stained with Coomassie blue.

SUPPLEMENTAL INFORMATION

Supplemental Information includes two tables and can be found with this article online at http://dx.doi.org/10.1016/j.str.2015.12.012.

AUTHOR CONTRIBUTIONS

J.S.K. and N.C.H. crystallized the protein and carried out analysis using X-ray diffraction. J.S.K., S.S., and N.C.H. analyzed the crystal structure of HlyD and performed assembly analysis. S.S., M.L., S.L., and K.L. prepared the samples for in vivo studies and performed functional analysis. J.S.K., S.S., and N.C.H. wrote the manuscript.

ACKNOWLEDGMENTS

This study was supported by NRF-2014R1A2A1A11050283 funded by the Ministry of Science, ITC, and Future Planning, Republic of Korea, and by the R&D Convergence Center Support Program funded by the Ministry for Food, Agriculture, Forestry and Fisheries, Republic of Korea, to N.C.H. This study made use of beamline 5C at PLS (Pohang, Republic of Korea).

Received: August 27, 2015
Revised: December 15, 2015
Accepted: December 16, 2015
Published: January 28, 2016

REFERENCES

Akama, H., Matsuura, T., Kashiwagi, S., Yoneyama, H., Narita, S., Tsukihara, T., Nakagawa, A., and Nakae, T. (2004). Crystal structure of the membrane fusion protein, MexA, of the multidrug transporter in *Pseudomonas aeruginosa*. J. Biol. Chem. *279*, 25939–25942.

Balakrishnan, L., Hughes, C., and Koronakis, V. (2001). Substrate-triggered recruitment of the TolC channel-tunnel during type I export of hemolysin by *Escherichia coli*. J. Mol. Biol. *313*, 501–510.

Bavro, V.N., Pietras, Z., Furnham, N., Perez-Cano, L., Fernandez-Recio, J., Pei, X.Y., Misra, R., and Luisi, B. (2008). Assembly and channel opening in a bacterial drug efflux machine. Mol. Cell *30*, 114–121.

Bhakdi, S., Muhly, M., and Fussle, R. (1984). Correlation between toxin binding and hemolytic activity in membrane damage by staphylococcal alpha-toxin. Infect. Immun. *46*, 318–323.

Cha, S.S., An, Y.J., Jeong, C.S., Kim, M.K., Lee, S.G., Lee, K.H., and Oh, B.H. (2012). Experimental phasing using zinc anomalous scattering. Acta Crystallogr. D Biol. Crystallogr. *68*, 1253–1258.

Choi, H.K., Park, N.Y., Kim, D.I., Chung, H.J., Ryu, S., and Choi, S.H. (2002). Promoter analysis and regulatory characteristics of vvhBA encoding cytolytic hemolysin of *Vibrio vulnificus*. J. Biol. Chem. *277*, 47292–47299.

Du, D., Wang, Z., James, N.R., Voss, J.E., Klimont, E., Ohene-Agyei, T., Venter, H., Chiu, W., and Luisi, B.F. (2014). Structure of the AcrAB-TolC multidrug efflux pump. Nature *509*, 512–515.

Echols, N., Grosse-Kunstleve, R.W., Afonine, P.V., Bunkoczi, G., Chen, V.B., Headd, J.J., McCoy, A.J., Moriarty, N.W., Read, R.J., Richardson, D.C., et al. (2012). Graphical tools for macromolecular crystallography in PHENIX. J. Appl. Crystallogr. *45*, 581–586.

Emsley, P., Lohkamp, B., Scott, W.G., and Cowtan, K. (2010). Features and development of Coot. Acta Crystallogr. D Biol. Crystallogr. *66*, 486–501.

Gerken, H., and Misra, R. (2004). Genetic evidence for functional interactions between TolC and AcrA proteins of a major antibiotic efflux pump of *Escherichia coli*. Mol. Microbiol. *54*, 620–631.

Higgins, M.K., Bokma, E., Koronakis, E., Hughes, C., and Koronakis, V. (2004). Structure of the periplasmic component of a bacterial drug efflux pump. Proc. Natl. Acad. Sci. USA *101*, 9994–9999.

Hinchliffe, P., Greene, N.P., Paterson, N.G., Crow, A., Hughes, C., and Koronakis, V. (2014). Structure of the periplasmic adaptor protein from a major facilitator superfamily (MFS) multidrug efflux pump. FEBS Lett. *588*, 3147–3153.

Kenny, B., Taylor, S., and Holland, I.B. (1992). Identification of individual amino acids required for secretion within the haemolysin (HlyA) C-terminal targeting region. Mol. Microbiol. *6*, 1477–1489.

Kim, H.M., Xu, Y., Lee, M., Piao, S., Sim, S.H., Ha, N.C., and Lee, K. (2010). Functional interrelationships between the AcrA hairpin tip region and the TolC aperture tip region for the formation of bacterial tripartite efflux pump AcrAB-TolC. J. Bacteriol. *192*, 4498–4503.

Kim, J.S., Jeong, H., Song, S., Kim, H.Y., Lee, K., Hyun, J., and Ha, N.C. (2015). Structure of the tripartite multidrug efflux pump AcrAB-TolC suggests an alternative assembly mode. Mol. Cells *38*, 180–186.

Koronakis, V., Sharff, A., Koronakis, E., Luisi, B., and Hughes, C. (2000). Crystal structure of the bacterial membrane protein TolC central to multidrug efflux and protein export. Nature *405*, 914–919.

Lee, M., Jun, S.Y., Yoon, B.Y., Song, S., Lee, K., and Ha, N.C. (2012). Membrane fusion proteins of type I secretion system and tripartite efflux pumps share a binding motif for TolC in gram-negative bacteria. PLoS One *7*, e40460.

Letoffe, S., Delepelaire, P., and Wandersman, C. (1996). Protein secretion in gram-negative bacteria: assembly of the three components of ABC protein-mediated exporters is ordered and promoted by substrate binding. EMBO J. *15*, 5804–5811.

Lewis, K. (2000). Translocases: a bacterial tunnel for drugs and proteins. Curr. Biol. *10*, R678–R681.

Liu, Q., Liu, Q., and Hendrickson, W.A. (2013). Robust structural analysis of native biological macromolecules from multi-crystal anomalous diffraction data. Acta Crystallogr. D Biol. Crystallogr. *69*, 1314–1332.

Lobedanz, S., Bokma, E., Symmons, M.F., Koronakis, E., Hughes, C., and Koronakis, V. (2007). A periplasmic coiled-coil interface underlying TolC recruitment and the assembly of bacterial drug efflux pumps. Proc. Natl. Acad. Sci. USA *104*, 4612–4617.

Mackman, N., and Holland, I.B. (1984). Functional characterization of a cloned haemolysin determinant from *E. coli* of human origin, encoding information for the secretion of a 107K polypeptide. Mol. Gen. Genet. *196*, 129–134.

Mikolosko, J., Bobyk, K., Zgurskaya, H.I., and Ghosh, P. (2006). Conformational flexibility in the multidrug efflux system protein AcrA. Structure *14*, 577–587.

Noegel, A., Rdest, U., Springer, W., and Goebel, W. (1979). Plasmid cistrons controlling synthesis and excretion of the exotoxin alpha-haemolysin of *Escherichia coli*. Mol. Gen. Genet. *175*, 343–350.

Otwinosky, Z., and Minor, W. (1997). Processing of X-ray diffraction data collected in oscillation mode. Methods Enzymol. *276*, 307–326.

Sauter, C., Basquin, J., and Suck, D. (2003). Sm-like proteins in Eubacteria: the crystal structure of the Hfq protein from *Escherichia coli*. Nucleic Acids Res. *31*, 4091–4098.

Schmitt, L., Benabdelhak, H., Blight, M.A., Holland, I.B., and Stubbs, M.T. (2003). Crystal structure of the nucleotide-binding domain of the ABC-transporter haemolysin B: identification of a variable region within ABC helical domains. J. Mol. Biol. *330*, 333–342.

Schulein, R., Gentschev, I., Schlor, S., Gross, R., and Goebel, W. (1994). Identification and characterization of two functional domains of the hemolysin translocator protein HlyD. Mol. Gen. Genet. *245*, 203–211.

Song, S., Kim, J.S., Lee, K., and Ha, N.C. (2015). Molecular architecture of the bacterial tripartite multidrug efflux pump focusing on the adaptor bridging model. J. Microbiol. *53*, 355–364.

Su, C.C., Yang, F., Long, F., Reyon, D., Routh, M.D., Kuo, D.W., Mokhtari, A.K., Van Ornam, J.D., Rabe, K.L., Hoy, J.A., et al. (2009). Crystal structure of the membrane fusion protein CusB from *Escherichia coli*. J. Mol. Biol. *393*, 342–355.

Su, C.C., Long, F., and Yu, E.W. (2011). The Cus efflux system removes toxic ions via a methionine shuttle. Protein Sci. *20*, 6–18.

Symmons, M.F., Bokma, E., Koronakis, E., Hughes, C., and Koronakis, V. (2009). The assembled structure of a complete tripartite bacterial multidrug efflux pump. Proc. Natl. Acad. Sci. USA *106*, 7173–7178.

Thanabalu, T., Koronakis, E., Hughes, C., and Koronakis, V. (1998). Substrate-induced assembly of a contiguous channel for protein export from *E. coli*: reversible bridging of an inner-membrane translocase to an outer membrane exit pore. EMBO J. *17*, 6487–6496.

Vagin, A., and Teplyakov, A. (2010). Molecular replacement with MOLREP. Acta Crystallogr. D Biol. Crystallogr. *66*, 22–25.

Wang, R.C., Seror, S.J., Blight, M., Pratt, J.M., Broome-Smith, J.K., and Holland, I.B. (1991). Analysis of the membrane organization of an Escherichia coli protein translocator, HlyB, a member of a large family of prokaryote and eukaryote surface transport proteins. J. Mol. Biol. *217*, 441–454.

Welch, R.A., Dellinger, E.P., Minshew, B., and Falkow, S. (1981). Haemolysin contributes to virulence of extra-intestinal *E. coli* infections. Nature *294*, 665–667.

Winn, M.D., Ballard, C.C., Cowtan, K.D., Dodson, E.J., Emsley, P., Evans, P.R., Keegan, R.M., Krissinel, E.B., Leslie, A.G., McCoy, A., et al. (2011). Overview of the CCP4 suite and current developments. Acta Crystallogr. D Biol. Crystallogr. *67*, 235–242.

Xu, Y., Sim, S.H., Song, S., Piao, S., Kim, H.M., Jin, X.L., Lee, K., and Ha, N.C. (2010). The tip region of the MacA alpha-hairpin is important for the binding to TolC to the *Escherichia coli* MacAB-TolC pump. Biochem. Biophys. Res. Commun. *394*, 962–965.

Xu, Y., Lee, M., Moeller, A., Song, S., Yoon, B.Y., Kim, H.M., Jun, S.Y., Lee, K., and Ha, N.C. (2011a). Funnel-like hexameric assembly of the periplasmic adapter protein in the tripartite multidrug efflux pump in gram-negative bacteria. J. Biol. Chem. *286*, 17910–17920.

Xu, Y., Song, S., Moeller, A., Kim, N., Piao, S., Sim, S.H., Kang, M., Yu, W., Cho, H.S., Chang, I., et al. (2011b). Functional implications of an intermeshing cogwheel-like interaction between TolC and MacA in the action of macrolide-specific efflux pump MacAB-TolC. J. Biol. Chem. *286*, 13541–13549.

Yum, S., Xu, Y., Piao, S., Sim, S.H., Kim, H.M., Jo, W.S., Kim, K.J., Kweon, H.S., Jeong, M.H., Jeon, H., et al. (2009). Crystal structure of the periplasmic component of a tripartite macrolide-specific efflux pump. J. Mol. Biol. *387*, 1286–1297.

Zgurskaya, H.I., Krishnamoorthy, G., Ntreh, A., and Lu, S. (2011). Mechanism and function of the outer membrane channel TolC in multidrug resistance and physiology of enterobacteria. Front. Microbiol. *2*, 189.